

## Unexpected fluorescence properties in the axially $\sigma$ -bonded ferrocenyl-containing porphyrin

Pavlo Solntsev,<sup>a</sup> Jared R. Sabin,<sup>a</sup> Samantha J. Dammer,<sup>a</sup> Nikolay N. Gerasimchuk<sup>b</sup> and Victor N. Nemykin<sup>\*a</sup>

### Supporting Information

#### Experimental section

**Materials and Physical Measurements.** All reactions were performed under dry nitrogen atmosphere with flame-dried glassware. Dry toluene was obtained by distillation over sodium, while dry DCM was obtained by distillation over calcium hydride prior experiments. All solvents used in column chromatography and reaction workups were purchased from commercially available sources and used without further purification. Silica gel (60 Å, 32 - 63 mesh) was purchased from Sorbent Technologies, basic aluminum oxide (Activity I, 58 Å, 150 mesh) was purchased from Fischer Inc.. For electrochemical experiments, anhydrous DCM was used without further purification. Tetrabutylammonium tetrakis(perfluorophenyl)borate (TFAB) was prepared according to the literature,<sup>15</sup> by metathesis reaction between lithium tetrakis(perfluorophenyl)borate and tetrabutylammonium bromide. NMR spectra were recorded on Varian INOVA instrument with 500 MHz frequency for protons and 125 MHz for carbon. Chemical shifts are reported in parts per million and referenced to TMS as an internal standard. UV-Vis data were obtained on Jasco-720 or Cary 17 spectrophotometers. MCD data were recorded

using OLIS DCM 17 CD spectropolarimeter using 1.4 T DeSa magnet. Electrochemical measurements were conducted using CH electrochemical analyzer utilizing three-electrode scheme with platinum working, auxiliary and reference electrodes in 0.05 M solution of TFAB in DCM with redox potentials corrected using internal standard (decamethylferrocene) in all cases. Spectroelectrochemical data were collected using home-build spectroelectrochemical cell in solution of 0.15 M solutions of TBAF in DCM. APCI-MS and APCI-MS/MS experiments were conducted using Advantage Max Finnegan LC-MS system.

**Computational Details.** All computations were performed using Gaussian 03<sup>1</sup> software package running under Windows or UNIX OS. The excitation energies were calculated by TDDFT approach with the lowest 150 singlet excited states been considered. In all calculations, Becke's exchange functional and Perdew-Wang correlation functional (BPW91) were used. Wachter's full-electron basis set was used for iron, DGauss DZVP basis set was used for tin atom, while for all other atoms 6-311G(d)<sup>2</sup> basis set was employed. The percentage of atomic orbital contributions to their respective molecular orbitals were calculated by using the VMOdes program.<sup>3</sup> In all cases, frequency calculations were performed to ensure that the optimized structures represent potential energy surface minima. It has been shown that BPW91 exchange-correlation functional coupled with the mentioned above basis set could accurately predict MLCT and  $\pi-\pi^*$  in variety of ferrocene-containing compounds, porphyrins, and phthalocyanines (see reference 14 of the main text). The typical errors for the TDDFT predicted by the mentioned above combination of the exchange-correlation functional and basis set method are within  $\sim 0.1$  eV.

**Preparation of *trans*-SnFc<sub>2</sub>TPP (2):** 233 mg (0.748 mmol) of iodoferrocene were dissolved in 6 ml of dry diethyl ether at room temperature and then cooled down to -78°C. 0.3 ml of 2.5M solution of butyl lithium in hexane was added dropwise with intensive stirring. After stirring at -78°C for 5 min, cold bath was removed and mixture was left to warm up to room temperature. At this time formation of orange solid of lithium ferrocene salt was observed. Suspension of ferrocenyl lithium was added as a one portion to a solution of SnCl<sub>2</sub>TPP (100 mg, 0.125 mmol) in 10 ml of dry toluene and the resulting solution immediately became green. Reaction mixture was stirred at room temperature for 24 h and then quenched with 1 ml of distilled water. All solvents were removed under vacuum and remained solid was washed with toluene. Toluene solution was chromatographed on aluminum column with toluene-dichloromethane-triethylamine (50:50:1) as eluent. Second green fraction was collected. Solvent was removed under vacuum. *Trans*-SnFc<sub>2</sub>TPP (2) was crystallized from toluene-hexane as green powder. Yield: 34 mg (25 %).

**Supporting Information Table 1.** Comparison of fluorescence quantum yields in ferrocene-containing porphyrins and reference compounds.

Porphyrin	Solvent	Fluorescence $\lambda_{\max}$ /nm ( $\Phi$ )	Literature
ZnTPP	EtOH	606, 656 (0.043)	a
ZnTPP	Toluene	(0.030)	b
ZnTPP	DCM	(0.022)	b
ZnPh <sub>3</sub> Fc <sub>1</sub> P	EtOH	not observed	a
[ZnPh <sub>3</sub> Fc <sub>1</sub> P] <sup>+</sup>	EtOH	610, 660 (0.006)	a
H <sub>2</sub> Ph <sub>3</sub> Fc <sub>1</sub> P	DCM	not observed	this work
<i>cis</i> -H <sub>2</sub> Ph <sub>2</sub> Fc <sub>2</sub> P	DCM	not observed	this work
<i>trans</i> -H <sub>2</sub> Ph <sub>2</sub> Fc <sub>2</sub> P	DCM	not observed	this work
H <sub>2</sub> PhFc <sub>3</sub> P	DCM	not observed	this work
H <sub>2</sub> TFcP	DCM	not observed	this work
<b>1</b>	DCM	607, 631, 660 (0.009)	this work
<b>2</b>	Toluene	651, 716 (0.003)	this work

a) J. Rochford, A. D. Rooney and M. T. Pryce, *Inorg. Chem.* 2007, **46**, 7247; b) J.-S. Hsiao, B. P. Krueger, R. W. Wagner, T. E. Johnson, J. K. Delaney, D. C. Mauzerall, G. R. Fleming, J. S. Lindsey, D. F. Bocian and R. J. Donohoe *J. Am. Chem. Soc.* 1996, **118**, 11181.

Selected crystallographic information for **2**:

Crystal Data collection and Refinement for <i>trans-SnFc<sub>2</sub>TPP</i> .	
Empirical formula	C <sub>64</sub> H <sub>46</sub> Fe <sub>2</sub> N <sub>4</sub> Sn
Formula weight	1101.48
Crystal system	Triclinic
Space group, Z	P <sup>1</sup> , 1
a (Å)	10.737(1)
b (Å)	11.288(1)
c (Å)	12.173(1)
α (°)	101.657(1)
β (°)	108.082(1)
γ (°)	115.058(1)
Volume (Å <sup>3</sup> )	1171.4(2)
ρ <sub>calc</sub> (g/cm <sup>3</sup> )	1.561
μ(Mo-K <sub>α</sub> )(mm <sup>-1</sup> )	1.189
θ <sub>max</sub> (°)	29.13
Reflections collected/unique, R <sub>int</sub>	16707 / 6273, 0.034
Data/restraints/parameters	6252 / 0 / 322
GooF(F <sup>2</sup> )	0.9889
R <sub>1</sub> <sup>a</sup> , wR <sub>2</sub> <sup>b</sup> (F <sup>2</sup> >2σ(F <sup>2</sup> ))	0.0354, 0.0901
R <sub>1</sub> <sup>a</sup> , wR <sub>2</sub> <sup>b</sup> (all data)	0.0485, 0.1059
Δρ <sub>max</sub> /Δρ <sub>min</sub> (e/Å <sup>3</sup> )	1.41 / -1.46
<sup>a</sup> R <sub>1</sub> (F) = Σ  F <sub>o</sub>   -  F <sub>c</sub>    / Σ F <sub>o</sub>  . <sup>b</sup> wR <sub>2</sub> (F <sup>2</sup> ) = {Σ[w(F <sub>o</sub> <sup>2</sup> - F <sub>c</sub> <sup>2</sup> ) <sup>2</sup> ] / Σw(F <sub>o</sub> <sup>2</sup> ) <sup>2</sup> } <sup>1/2</sup> . w <sup>1/2</sup> = [1.0/(2.14*t[0]'(x)+2.62*t[1]'(x)+0.644*t[2]'(x))] <sup>1/2</sup> , x = F <sub>o</sub> /F <sub>o</sub> <sup>max</sup>	

Selected bond distances (Å) for <i>trans-SnFc<sub>2</sub>TPP</i> .			
Sn(1)-N(2)	2.131(2)	C(17)-C(22)	1.399(4)
Sn(1)-N(1)	2.132(2)	C(18)-C(19)	1.391(4)
Sn(1)-C(23)	2.186(3)	C(19)-C(20)	1.389(5)
N(1)-C(1)	1.365(3)	C(20)-C(21)	1.382(4)
N(1)-C(4)	1.367(3)	C(21)-C(22)	1.389(4)
N(2)-C(6)	1.368(3)	C(23)-C(24)	1.439(4)
N(2)-C(9)	1.371(3)	C(23)-C(27)	1.427(4)
C(1)-C(10) <sup>a</sup>	1.417(4)	C(24)-C(25)	1.424(4)
C(1)-C(2)	1.456(4)	C(25)-C(26)	1.416(5)
C(2)-C(3)	1.366(4)	C(26)-C(27)	1.425(4)
C(3)-C(4)	1.445(4)	C(28)-C(29)	1.414(6)
C(4)-C(5)	1.416(4)	C(28)-C(32)	1.426(7)
C(5)-C(11)	1.501(3)	C(29)-C(30)	1.415(5)
C(5)-C(6)	1.417(4)	C(30)-C(31)	1.423(5)
C(6)-C(7)	1.447(3)	C(31)-C(32)	1.413(6)
C(7)-C(8)	1.361(4)	Fe(1)-C(23)	2.084(3)
C(8)-C(9)	1.447(3)	Fe(1)-C(24)	2.054(3)
C(9)-C(10)	1.422(4)	Fe(1)-C(25)	2.041(3)
C(10)-C(17)	1.497(3)	Fe(1)-C(26)	2.042(3)

C(11)-C(12)	1.392(4)	Fe(1)-C(27)	2.052(3)
C(11)-C(16)	1.394(4)	Fe(1)-C(28)	2.047(4)
C(12)-C(13)	1.398(4)	Fe(1)-C(29)	2.062(4)
C(13)-C(14)	1.381(4)	Fe(1)-C(30)	2.053(3)
C(14)-C(15)	1.382(4)	Fe(1)-C(31)	2.049(4)
C(15)-C(16)	1.397(4)	Fe(1)-C(32)	2.040(4)
C(17)-C(18)	1.398(4)		
a) -x, -y, 1-z			

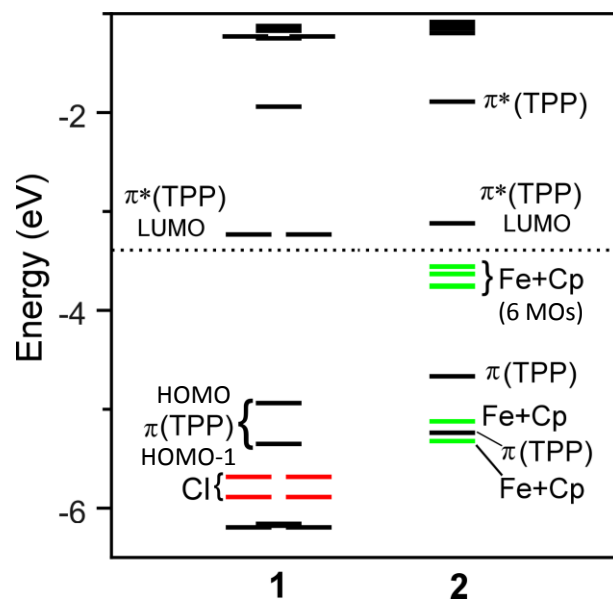
Selected bond angles (°) for <i>trans-SnFc<sub>2</sub>TPP</i> .			
C(23)a-Sn(1)-N(1)	85.90(9)	C(27)-C(23)-Fe(1)	68.6(2)
C(23)-Sn(1)-N(1)	94.10(9)	C(23)-C(24)-Fe(1)	70.8(2)
C(23)-Sn(1)-N(2) <sup>a</sup>	92.22(10)	C(25)-C(24)-Fe(1)	69.2(2)
C(23)-Sn(1)-N(2)	87.78(10)	C(24)-C(25)-Fe(1)	70.1(2)
N(1) <sup>a</sup> -Sn(1)-N(2)	89.92(8)	C(26)-C(25)-Fe(1)	69.7(2)
N(1)-Sn(1)-N(2)	90.08(8)	C(25)-C(26)-Fe(1)	69.7(2)
C(9)-N(2)-C(6)	109.2(2)	C(27)-C(26)-Fe(1)	70.0(2)
C(4)-N(1)-C(1)	109.3(2)	C(23)-C(27)-Fe(1)	71.0(2)
C(9)-N(2)-Sn(1)	124.5(2)	C(26)-C(27)-Fe(1)	69.3(2)
C(6)-N(2)-Sn(1)	124.3(2)	C(32)-C(28)-Fe(1)	69.3(2)
C(4)-N(1)-Sn(1)	124.9(2)	C(29)-C(28)-Fe(1)	70.4(2)
C(1)-N(1)-Sn(1)	125.6(2)	C(30)-C(29)-Fe(1)	69.5(2)
C(24)-C(23)-Sn(1)	125.9(2)	C(28)-C(29)-Fe(1)	69.3(2)
C(27)-C(23)-Sn(1)	126.6(2)	C(31)-C(30)-Fe(1)	69.6(2)
Fe(1)-C(23)-Sn(1)	140.1(1)	C(29)-C(30)-Fe(1)	70.2(2)
C(10) <sup>a</sup> -C(1)-C(2)	126.7(2)	C(30)-C(31)-Fe(1)	69.8(2)
C(10) <sup>a</sup> -C(1)-N(1)	125.6(2)	C(32)-C(31)-Fe(1)	69.4(2)
C(2)-C(1)-N(1)	107.7(2)	C(28)-C(32)-Fe(1)	69.8(2)
C(1)-C(2)-C(3)	107.5(2)	C(31)-C(32)-Fe(1)	70.1(2)



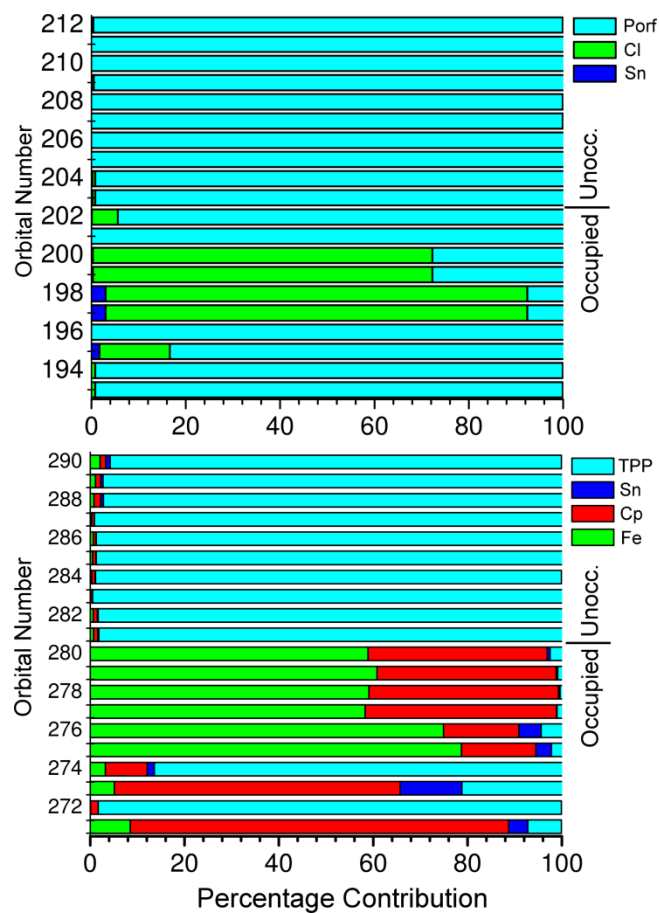
C(4)-C(3)-C(2)	107.2(2)	C(23)-Fe(1)-C(29)	148.6(1)
C(5)-C(4)-C(3)	125.9(2)	C(23)-Fe(1)-C(24)	40.7(1)
C(5)-C(4)-N(1)	125.8(2)	C(29)-Fe(1)-C(24)	116.3(2)
C(3)-C(4)-N(1)	108.3(2)	C(23)-Fe(1)-C(30)	170.4(1)
C(6)-C(5)-C(4)	127.8(2)	C(29)-Fe(1)-C(30)	40.2(2)
C(6)-C(5)-C(11)	115.9(2)	C(24)-Fe(1)-C(30)	147.6(1)
C(4)-C(5)-C(11)	116.3(2)	C(23)-Fe(1)-C(27)	40.4(1)
C(5)-C(6)-C(7)	125.7(2)	C(29)-Fe(1)-C(27)	169.5(2)
C(5)-C(6)-N(2)	126.3(2)	C(24)-Fe(1)-C(27)	67.5(1)
C(7)-C(6)-N(2)	107.9(2)	C(30)-Fe(1)-C(27)	131.6(1)
C(6)-C(7)-C(8)	107.5(2)	C(23)-Fe(1)-C(31)	131.7(1)
C(9)-C(8)-C(7)	107.5(2)	C(29)-Fe(1)-C(31)	68.2(2)
C(10)-C(9)-C(8)	126.0(2)	C(24)-Fe(1)-C(31)	171.0(1)
C(10)-C(9)-N(2)	126.2(2)	C(30)-Fe(1)-C(31)	40.6(1)
C(8)-C(9)-N(2)	107.8(2)	C(27)-Fe(1)-C(31)	109.7(2)
C(1) <sup>a</sup> -C(10)-C(9)	127.6(2)	C(23)-Fe(1)-C(28)	116.7(1)
C(1) <sup>a</sup> -C(10)-C(17)	116.2(2)	C(29)-Fe(1)-C(28)	40.3(2)
C(9)-C(10)-C(17)	116.2(2)	C(24)-Fe(1)-C(28)	109.0(2)
C(5)-C(11)-C(12)	121.7(2)	C(30)-Fe(1)-C(28)	68.1(2)
C(5)-C(11)-C(16)	119.0(2)	C(27)-Fe(1)-C(28)	149.6(2)

C(12)-C(11)-C(16)	119.3(2)	C(23)-Fe(1)-C(26)	68.9(1)
C(11)-C(12)-C(13)	120.0(3)	C(29)-Fe(1)-C(26)	130.1(2)
C(12)-C(13)-C(14)	120.2(3)	C(24)-Fe(1)-C(26)	68.1(1)
C(13)-C(14)-C(15)	120.2(3)	C(30)-Fe(1)-C(26)	108.0(1)
C(14)-C(15)-C(16)	119.9(3)	C(27)-Fe(1)-C(26)	40.7(1)
C(15)-C(16)-C(11)	120.3(3)	C(23)-Fe(1)-C(25)	69.1(1)
C(10)-C(17)-C(18)	120.8(2)	C(29)-Fe(1)-C(25)	107.8(2)
C(10)-C(17)-C(22)	120.4(2)	C(24)-Fe(1)-C(25)	40.7(1)
C(18)-C(17)-C(22)	118.8(2)	C(30)-Fe(1)-C(25)	114.9(1)
C(17)-C(18)-C(19)	120.1(3)	C(27)-Fe(1)-C(25)	68.1(1)
C(18)-C(19)-C(20)	120.5(3)	C(23)-Fe(1)-C(32)	110.1(1)
C(19)-C(20)-C(21)	119.8(3)	C(29)-Fe(1)-C(32)	67.6(2)
C(20)-C(21)-C(22)	120.1(3)	C(24)-Fe(1)-C(32)	132.5(2)
C(17)-C(22)-C(21)	120.7(3)	C(30)-Fe(1)-C(32)	67.6(2)
C(24)-C(23)-C(27)	105.3(3)	C(27)-Fe(1)-C(32)	118.0(2)
C(23)-C(24)-C(25)	109.5(3)	C(31)-Fe(1)-C(28)	68.9(2)
C(24)-C(25)-C(26)	107.7(3)	C(31)-Fe(1)-C(26)	115.7(2)
C(25)-C(26)-C(27)	107.6(3)	C(28)-Fe(1)-C(26)	168.6(2)
C(23)-C(27)-C(26)	109.9(3)	C(31)-Fe(1)-C(25)	147.3(1)
C(32)-C(28)-C(29)	106.8(4)	C(28)-Fe(1)-C(25)	130.1(2)

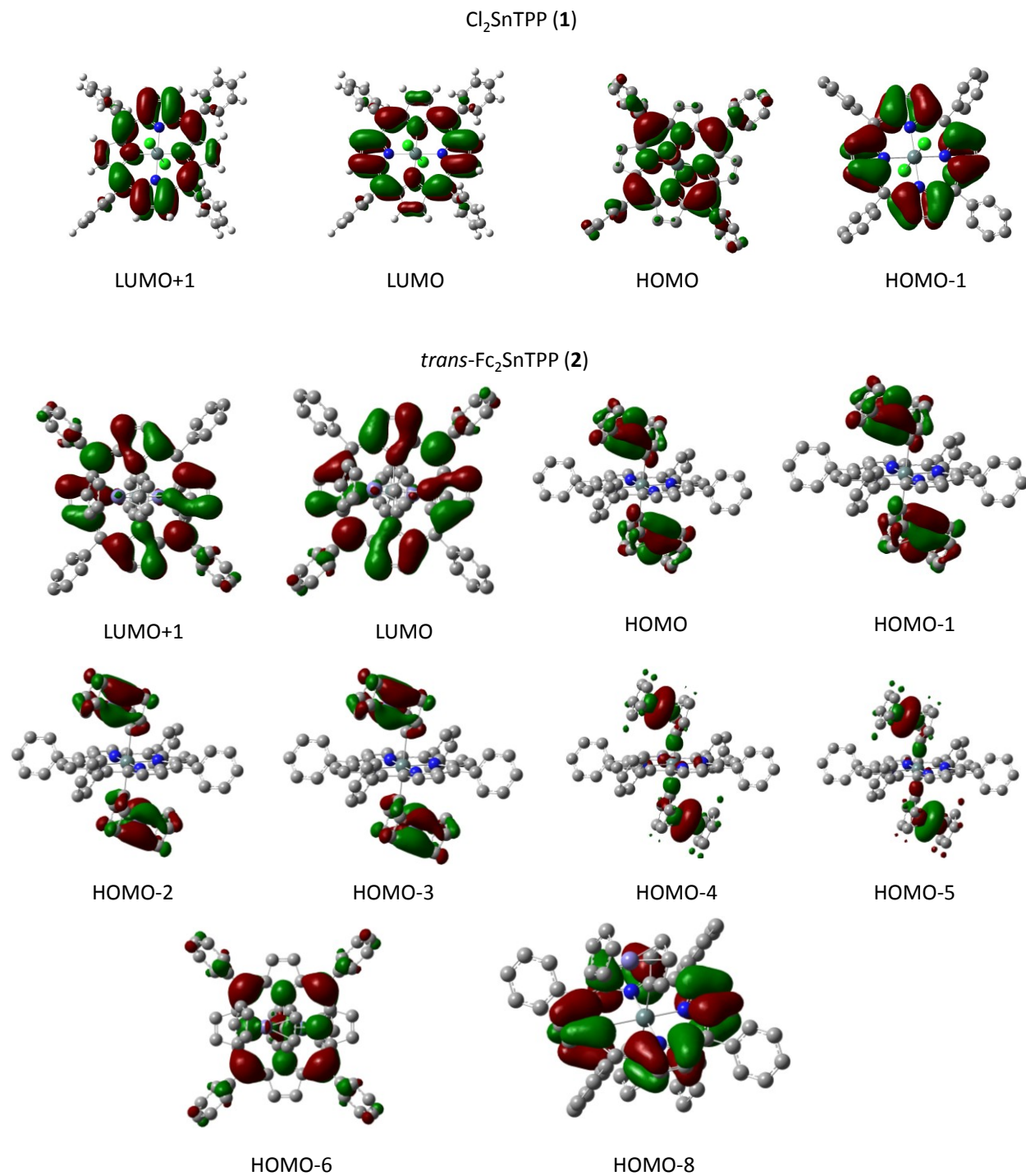
C(30)-C(29)-C(28)	108.5(4)	C(26)-Fe(1)-C(25)	40.6(1)
C(31)-C(30)-C(29)	108.5(3)	C(31)-Fe(1)-C(32)	40.4(2)
C(32)-C(31)-C(30)	106.8(4)	C(28)-Fe(1)-C(32)	40.8(2)
C(28)-C(32)-C(31)	109.3(4)	C(26)-Fe(1)-C(32)	148.9(2)
C(24)-C(23)-Fe(1)	68.5(2)	C(25)-Fe(1)-C(32)	170.2(2)
a) -x, -y, 1-z			



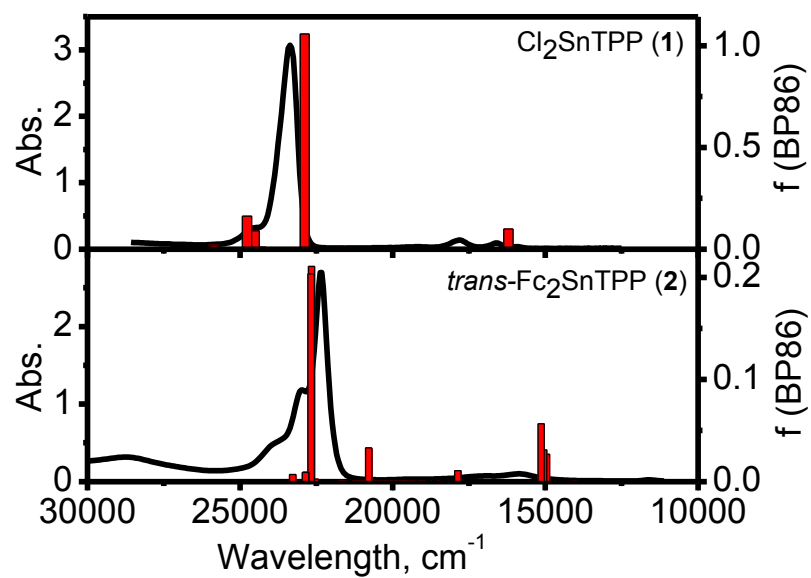
**Supporting Information Figure 1.** Molecular orbital energy diagram for complexes **1** and **2** calculated at DFT level.



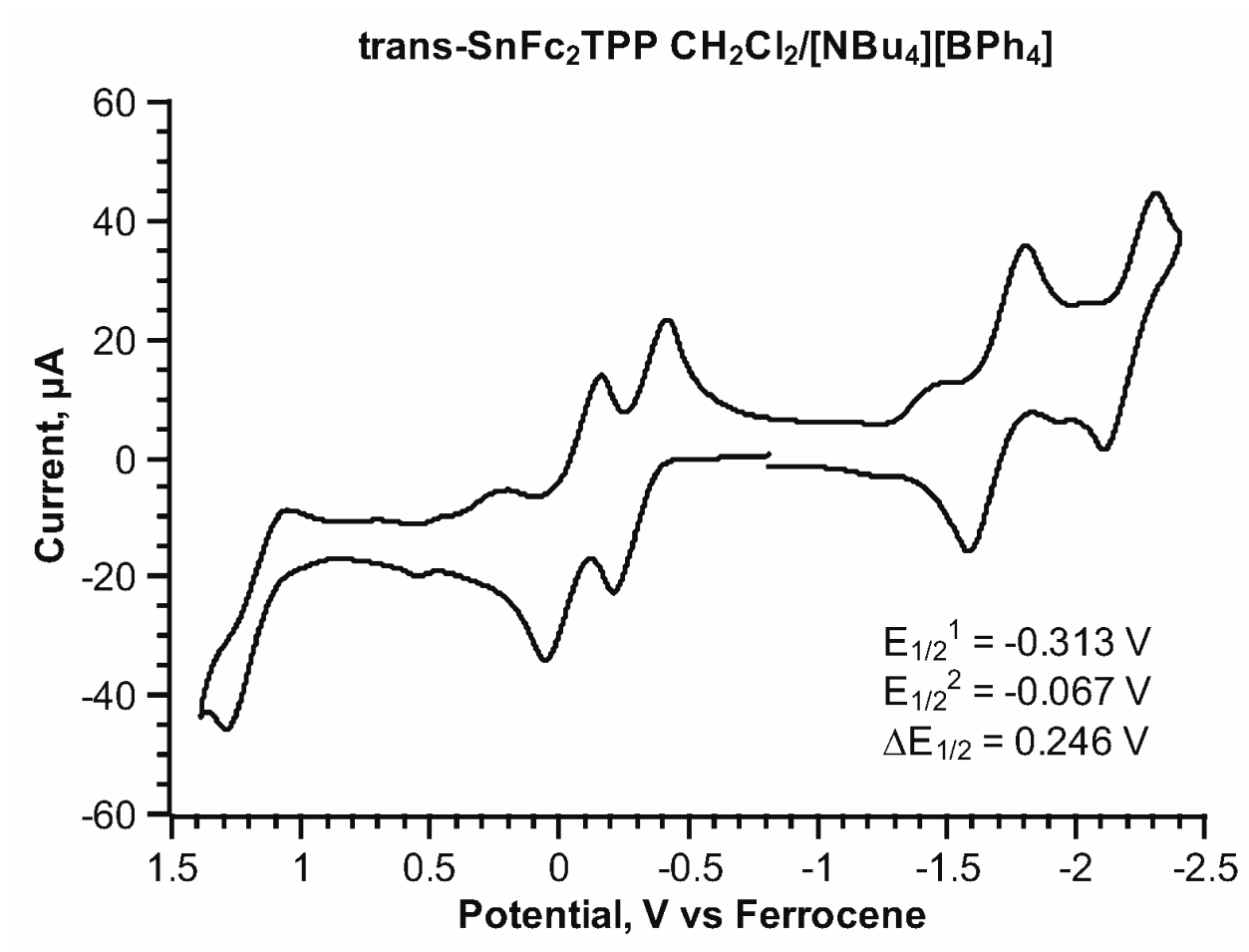
**Supporting Information Figure 2a.** Molecular orbital composition for complexes **1** and **2** calculated at DFT level.



**Supporting Information Figure 2b.** Selected molecular orbitals of complexes **1** and **2** calculated at DFT level.

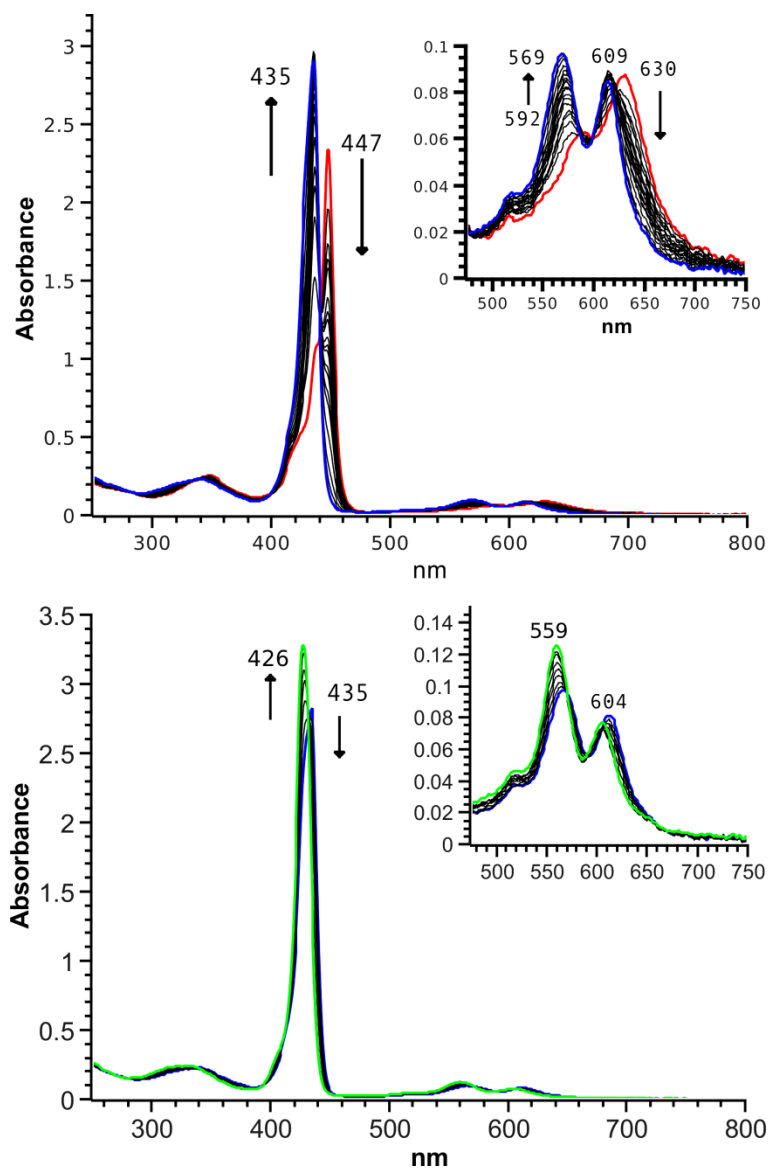


**Supporting Information Figure 3.** Comparison between TDDFT calculated vertical excitation energies of **1** and **2** (vertical red bars) and their experimental data (black lines).

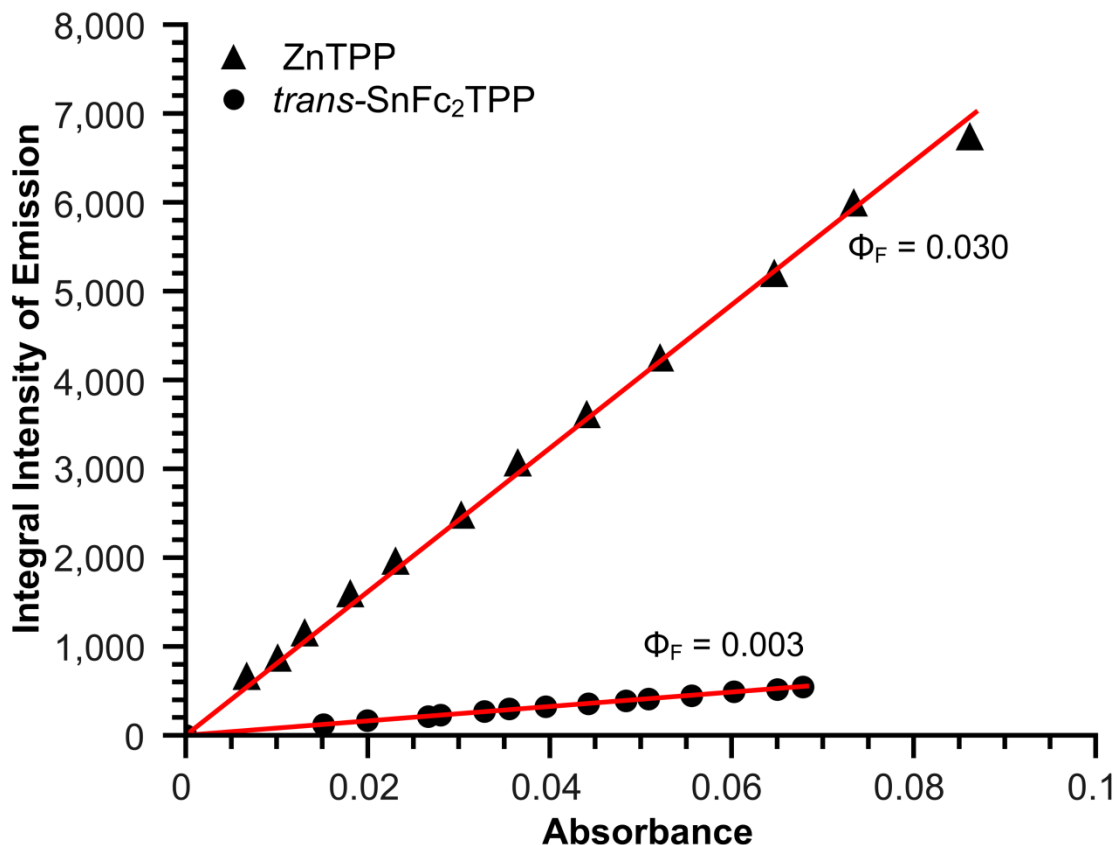


**Supporting Information Figure 4.** CV of complex **2** in DCM/TFAB system at 100 mV/s. Potentials (Fc/Fc<sup>+</sup>): +1.17 V; -0.07 V; -0.31 V; -1.70 V, and -2.21 V.





**Supporting Information Figure 5.** Stepwise oxidative transformation of **2** into **2<sup>+</sup>** (top) and **2<sup>+</sup>** into **2<sup>2+</sup>** (bottom) in DCM.



Supporting Information Figure 6. Quantum yield determination curves for **2** in toluene.

<sup>1</sup> Frisch, M. J.; Trucks, G. W.; Schlegel, H. B.; Gill, P. M. W.; Johnson, B. G.; Robb, M. A.; Cheeseman, J. R.; Keith, T. A.; Petersson, G. A.; Montgomery, J. A.; Raghavachari, K.; Al-Laham, M. A.; Zakrzewski, V. G.; Ortiz, J. V.; Foresman, J. B.; Cioslowski, J.; Stefanov, B. B.; Nanayakkara, A.; Challacombe, M.; Peng, C. Y.; Ayala, P. Y.; Chen, W.; Wong, M. W.; Andres, J. L.; Replogle, E. S.; Gomperts, R.; Martin, R. L.; Fox, D. J.; Binkley, J. S.; Defrees, D. J.; Baker, J.; Stewart, J. P.; Head-Gordon, M.; Gonzalez, C.; Pople, J. A. *Gaussian 98* (Gaussian, Inc., Pittsburgh, PA, 1998).

<sup>2</sup> McLean, A. D.; Chandler, G. S. *J. Chem. Phys.* **1980**, *72*, 5639; Krishnan, R.; Binkley, J. S.; Seeger, R.; Pople, J. A. *J. Chem. Phys.* **1980**, *72*, 650.

<sup>3</sup> Nemykin, V. N.; Basu, P. VModes: Virtual Molecular Orbital description program for Gaussian, GAMESS, and HyperChem, Revision A 7.1, 2003.